

Analysis and verification of stresses in reinforced concrete bridge projects of the box type with sequential application of prestress based on the successive advancement method

Análise e verificação de tensões em projectos de pontes de concreto armado de tipo caixão com aplicação sequencial de pré-esforço com base no método dos avanços sucessivos

Análisis y verificación de tensiones en proyectos de puentes de hormigón armado del tipo cajón con aplicación secuencial de pretensado basado en el método de avance sucesivo

Received: 11/19/2023 | Reviewed: 01/09/2024 | Accepted: 01/10/2024 | Published: 02/03/2024

Eleutério Zeferino

National Institute of Roads in Angola, Angola

Medci Kahenda Silva

Higher Polytechnic Institute of Technology and Sciences, Angola

Akihito Boa Esperança

Higher Polytechnic Institute of Technology and Sciences, Angola

José Paulo Kai

Jean Piaget University of Angola, Angola

Agostinho Neto University, Angola

Vencislau Quissanga

ORCID: <https://orcid.org/0000-0003-4746-1974>

Higher Polytechnic Institute of Technology and Sciences, Angola

E-mail: vencislau.quissanga@ispotec.co.ao

Abstract

Given the importance of road bridge systems for the development of a country, rigor in the design process becomes extremely essential in order to meet all requirements related to their functionality. One of the challenging aspects of avoiding possible collapse problems at the beginning or during the construction phase of the project is the selection of the construction process. In this context, the criteria for defining the construction process to be adopted is intrinsically linked to cost, ease of execution, and safety during the creation of the work of art, construction time and the technical capacity of the construction professionals. In this study, deformation analyses and the evolution of efforts in the upper fibers of a bridge were carried out based on conventional construction methods, taking into account the application of pre-stress during construction, aiming to compare the results. Highlighting that the critical tensions were overcome with the help of applying pre-stress in a phased and/or sequential manner. The structural system in question is a single-cell box bridge made of pre-stressed concrete with variable height, measuring 2.50 m in the middle of the span and 4.70 m at the supports. The computational numerical modelling was developed based on the use of finite element programs CSiBridge v.20 and Robot Structural, considering bar and plate/shell/shell elements. Using the method of successive symmetric advances, a longitudinal, linear-static analysis was carried out (neglecting dynamic effects), taking into account the zero, corresponding and closing staves with length measurements of 6.40 m, 4.20 m and 3.00 m, respectively. The results were compared, where it was concluded that the efforts obtained in the construction phase after closing the consoles turned out to be relatively lower due to the redistribution of efforts, taking into account the change in the structural system from isostatic to hyperstatic. With this change, tensile stresses appeared in the lower fibers (this during the construction phase), increasing by 92.10% during the operation phase. The tensile efforts of the upper fibers in the support area increased by 85.6% from the construction phase to the operation phase. Regarding the pre-stressing strength of the concrete, it was applied in order to guarantee reduced losses resulting in values lower than 15%.

Keywords: Reinforced concrete bridge; Box beam; Pre-stress; Successive advances; Staves; Pre-stress cables.

Resumo

Dada a importância dos sistemas de pontes rodoviárias para o desenvolvimento de um país, torna-se extremamente fundamental o rigor no processo de concepção de modo a atender todas as exigências correlatas a sua funcionalidade. Um dos aspectos desafiadores para evitar possíveis problemas de colapso logo no início ou na fase construtiva de projeto é a seleção do processo construtivo. Nesse contexto, os critérios para a definição do processo construtivo a ser adotado estão intrinsecamente ligados com o custo, facilidade de execução, segurança durante a realização da obra de arte, tempo de construção e a capacidade técnica dos profissionais da obra. Neste estudo, realizou-se as análises de deformações e a evolução dos esforços nas fibras superiores de uma ponte com base nos métodos construtivos convencionais, tendo

em conta a aplicação do pré-esforço durante a construção, objetivando comparar os resultados. Destacando que as tensões críticas, foram colmatadas com o auxílio da aplicação do pré-esforço de forma faseada e/ou sequencial. O sistema estrutural em questão, trata-se de uma ponte caixão unicelular de betão pré-esforçado com altura variável, tendo 2,50 m no centro do vão e 4,70 m nos apoios. As modelagens numéricas computacionais foram desenvolvidas com base na utilização dos programas de elementos finitos CSiBridge e o Robot Structural, considerando os elementos de tipo barra, área e de plano. Com o método dos avanços sucessivos de forma simétrica, foi realizada a análise longitudinal, lineal-estática (desprezando os efeitos dinâmicos), tendo em conta as aduelas zero, correspondentes e de fecho com as medidas de comprimento de 6,40 m, 4,20 m e 3,00 m, respectivamente. Realizou-se a comparação dos resultados, onde concluiu-se que os esforços obtidos na fase construtiva após o fecho das consolas resultaram ser relativamente mais baixos devido a redistribuição dos esforços, tendo em conta a mudança no sistema estrutural de isostático para hiperestático. Com esta mudança surgiram as tracções nas fibras inferiores (isso na fase construtiva), aumentando em 92,10% durante a fase operação. Os esforços de tracção das fibras superiores na zona dos apoios aumentaram em 85,6% da fase construtiva à fase de operação. Relativamente à força de pré-esforço do betão, aplicou-se de modo a garantir perdas reduzidas resultando em valores menores que 15%.

Palavras-chave: Ponte de concreto armado; Viga caixão; Pré-esforço; Avanços sucessivos; Aduelas.

Resumen

Dada la importancia de los sistemas de puentes viales para el desarrollo de un país, el rigor en el proceso de diseño se vuelve sumamente esencial para cumplir con todos los requisitos relacionados con su funcionalidad. Uno de los aspectos desafiantes para evitar posibles problemas de colapso al inicio o durante la fase de construcción del proyecto es la selección del proceso constructivo. En este contexto, los criterios para definir el proceso constructivo a adoptar están intrínsecamente ligados al costo, la facilidad de ejecución y la seguridad durante la creación de la obra de arte, el tiempo de construcción y la capacidad técnica de los profesionales de la construcción. En este estudio se realizaron análisis de deformación y evolución de esfuerzos en las fibras superiores de un puente con base en métodos constructivos convencionales, teniendo en cuenta la aplicación de pretensado durante la construcción, con el objetivo de comparar los resultados. Resaltando que las tensiones críticas fueron superadas con la ayuda de la aplicación de pretensado de manera escalonada y/o secuencial. El sistema estructural en cuestión es un puente cajón unicelular de hormigón pretensado de altura variable, con unas medidas de 2,50 m en la mitad del vano y 4,70 m en los apoyos. El modelado numérico computacional se desarrolló con base en el uso de los programas de elementos finitos CSiBridge v.20 y Robot Structural, considerando elementos barra y placa/cáscara/cáscara. Utilizando el método de avances simétricos sucesivos, se realizó un análisis lineal-estático longitudinal (despreciando efectos dinámicos), teniendo en cuenta las duelas cero, correspondiente y de cierre con medidas de longitud de 6,40 m, 4,20 m y 3,00 m, respectivamente. Se compararon los resultados, donde se concluyó que los esfuerzos obtenidos en la fase de construcción luego del cierre de las consolas resultaron ser relativamente menores debido a la redistribución de esfuerzos, teniendo en cuenta el cambio del sistema estructural de isostático a hiperestático. Con este cambio aparecieron esfuerzos de tracción en las fibras inferiores (esto durante la fase de construcción), incrementándose en un 92,10% durante la fase de operación. Los esfuerzos de tracción de las fibras superiores en la zona de soporte aumentaron un 85,6% desde la fase de construcción hasta la fase de operación. En cuanto a la resistencia del pretensado del hormigón, se aplicó con el fin de garantizar pérdidas reducidas resultando en valores inferiores al 15%.

Palabras-clave: Puente de hormigón armado; Viga cajón; Pretensado; Avances sucesivos; Duelas; Cables pretensados.

1. Introduction

Regarding studies and/or developments in different locations, bridges have always been assumed as indicators for economic development. As we know, for its correct design, even taking into account the economic aspects, it is necessary that the requirements related to functionality (traffic) are met or fulfilled, ensuring that the constituent materials resist the stresses requested (ensuring safety), as well as correct structural behaviour, taking into account, above all, vibrations due to the passage of vehicles (in the particular case of bus stations) so that the structural system meets the useful life predicted in its design phase. To this end, it is important that the structural parts that make up the system are rigorously defined.

Even though construction processes have achieved significant advances over the years, it appears that most bridge structure collapses occur during the construction phase (Almeida, 2016; Barbaros et al., 2022; Briseghella et al., 2021; Cardoso, 2014 and Cardoso, 2015). Therefore, there is a strict need to adopt carefully developed study criteria to mitigate known problems in the bridge sector.

Various scholars have carried out numerous studies on the effects of optimizing construction taking into account stresses in the structural system. It is important to note that Davide et al. (2022) compared four methods when applied to analyse the

impact of loading on deformations and stresses of bridge structures. In the case of authors Chen et al. (2017), they proposed the force balance method to determine the initial stresses in reinforced concrete decks subjected to different loads, resulting in a reasonable distribution of bending moments (under the deck). Huang et al. (2019) studied the (long-term) performance of bridges built based on different methods affected by reinforced concrete shrinkage and creep.

As discussed above, decision-making on which construction method to adopt results from an in-depth analysis of several conditioning factors, such as: ease of execution (technical feasibility), cost, safety (during the process and/or carrying out of the bridge), construction time, technical capacity of professionals and others (Quissanga et al., 2021; 2022; Reis and Peres, 2016; Zhou et al., 2019).

In this context, in the case of reinforced concrete bridges with considerably large spans, these should be designed based on the most viable execution solutions, among which is the (quite efficient) solution that consists of adopting a box-beam section of one or more cells. The solution in question provides numerous benefits in the execution process, such as high rigidity, high resistance to bending and torsion, durability and ease in the process of future maintenance and/or inspections (Da Silva et al, 2023; Paixão, 2015; Motter et al., 2018; Fatemi et al. 2016; Davide et al., 2022).

The method of successive advances is quite advantageous compared to the others, due to the fact that it provides speed in the execution process and the possibility of eliminating false work supported on the ground, also giving the possibility of crossing large valleys and lakes with high depths without the need to interrupt traffic or navigation during the construction phase (Chai et al., 2019). However, the method in question makes it possible to carry out several or different work fronts (several spans simultaneously) to at the end or later join the referred spans (closing of consoles), thus making a much more economical and less time-consuming work carried out in a very short time, however demanding a rigorously specialized workforce, so that the cantilevers of the different spans are on the same alignment at the time of joining.

However, it is also important to mention that due to the existence of several actors involved in the construction process, it is often difficult to collect all the information produced and analyse the results obtained in the different phases of the project, therefore not becoming possible to draw conclusions about the differences in the results obtained and which reveal the evolution of the process, namely about the quantification and accounting of the requesting actions, the characteristics of construction materials, and also about the evolution of the calculation models used, thus evaluating, the differences and draw the appropriate conclusions.

Reinforced concrete bridges constructed using this method are typically constructed using a single-segment construction sequence, which involves first one or two segments being lifted and then the remaining segments installed also by lifting one at a time. Therefore, the present research work is intended to analyse and evaluate the structural stresses following (or in the process of) the application of pre-stresses during the construction of a reinforced concrete bridge with a box girder section, based on the use of the methodology of successive advances, which will be presented as a proposal for the bridge to be built on the Congo River or also called the Zaire River located in the north of Angola.

The computational numerical model investigated corresponds to a road structure with a deck and single-cell box beam with variable height of reinforced concrete in a parabolic shape, with a straight axis presenting 5 continuous spans (free spans) of 40.0 m at the ends, 55.0 m intermediate spans and a central span of 85.0 m, thus adding up to a 275.0 m bridge length. It is important to note that in this work, the usual mesh refinement techniques presented in simulations carried out with the aid of the finite element method implemented in the CSiBridge v.20 and Robot Structural software's were adopted.

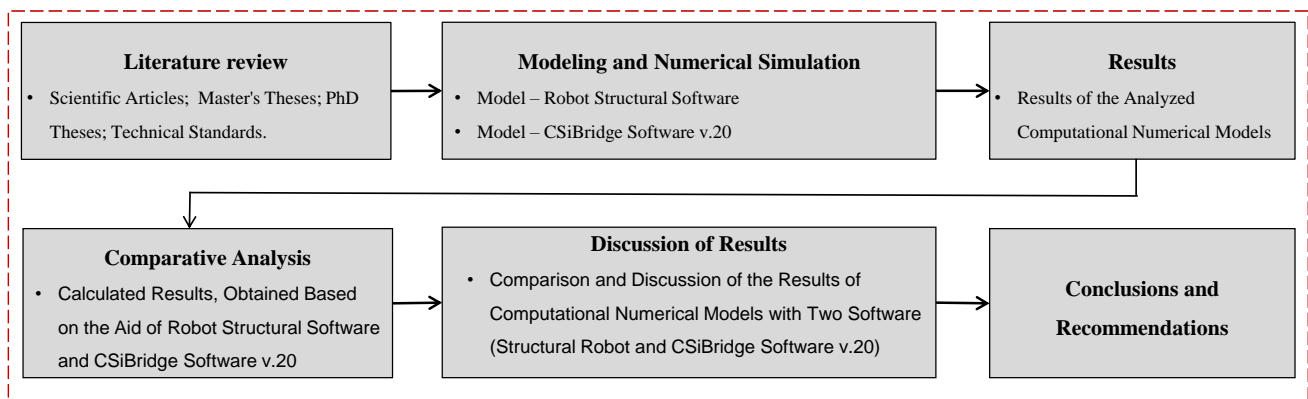
The results of the analyses are presented with the aim of verifying the deformations generated through the application of pre-stresses in a sequenced manner during the construction process. Therefore, the main conclusions of the study in question are intended to alert structural engineers about one of the most viable and recommended methodologies for the construction of bridges with large spans subjected to load actions.

2. Methodology

This research work was prepared through a comparative analysis of a computational numerical study, using the qualitative method, which helps to better understand phenomena rigorously studied in isolation. As for the theoretical foundation, it was structured based on technical regulations for the design of reinforced concrete bridges and viaducts (Eurocode 1, 2010; NBR 7188: ABNT, 2021). It is important to note that in addition to the concepts focused on cantilever bridge analysis methods formulated by Bakht & Jaeger (1985), the updates developed by the authors Bakht e Mufti (2015) were also taken into account.

As already mentioned, the numerical models were developed and simulated with the aid of CSiBridge v.20 and Robot Structural software in order to streamline the comparison and facilitate the extraction of the set of results for each case analysed. The comparison of the results of the numerical models used in this research are illustrated in item 5. Noting that the process of organization and understanding of this study occurs through the comparative analysis of the results obtained in the simulation of bridge slabs taking into account the staves and the pre- effort with the help of the aforementioned software; which are programs based on the finite element method. However, to obtain and organize the calculation results for the bridge slabs, the different thickness ratios of the deck structures were considered. In other words, based on the results obtained, the analyses were presented, comparative discussions were inferred and finally the conclusions and recommendations of the study, according to the flowchart presented in Figure 1.

Figure 1 - Flowchart of activities developed during the preparation of the research.



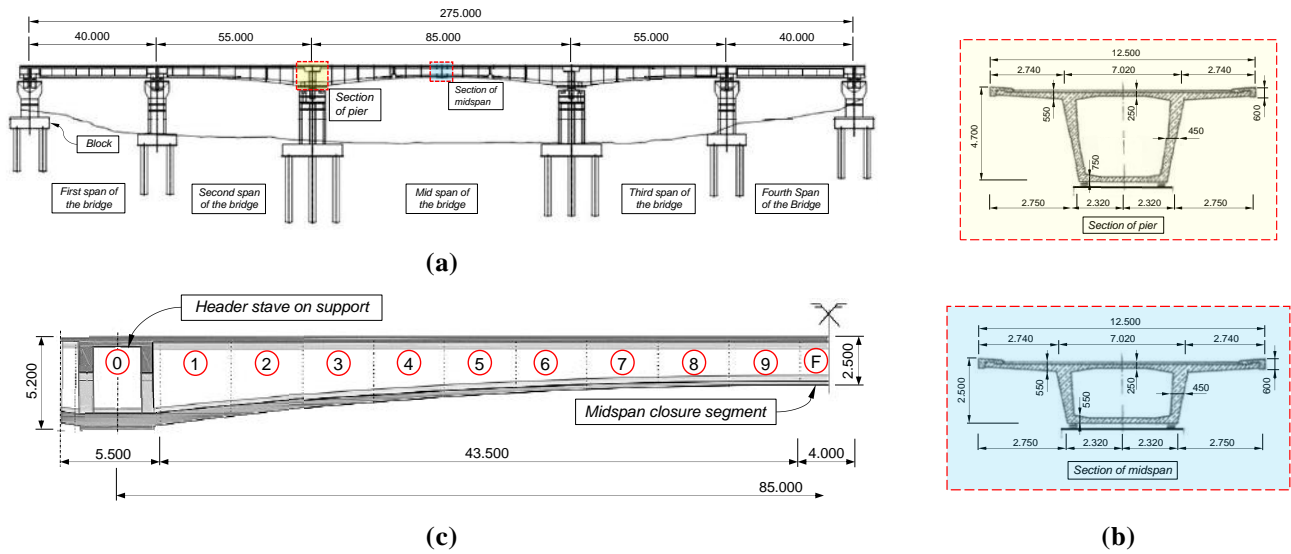
Source: Authors.

3. Highway Bridge Investigated

3.1 Coffin Type Bridges

The structural model of the reinforced concrete bridge investigated corresponds to a typical system composed of a deck and box beam with a straight axis (continuous), with a variable height of 2.50 m in the middle of the span and 4.70 m at the supports, with the main span of 275.0 m, and with span arrangements of 40.0 + 55.0 + 85.0 + 55.0 + 40.0 m, respectively. As can be seen in Figure 2, the bridge's structural system has a symmetrical arrangement of four pillars. The bridge deck has a total width of 12.50 m, with a bidirectional transverse slope of the slab of 2.5%. The characteristics of the materials used in the bridge in question are described in Table 1 below.

Figure 2 - Layout and dimensions of the bridge: (a) Longitudinal view of the bridge, b) Cross section of 1/2 of the bridge's main beam and (c) schematic diagram of precast segments of the main span. (Unit: mm).



Source: Authors.

Table 1 - Geometric and physical characteristics of the investigated reinforced concrete bridge.

Element	Description	
Prestress cables	Each cable defined for prestressing consists of a strand of 7 wires/tensioners with a nominal diameter of 15 mm (ASTM 0.6) and an area of 1.4cm ² , totalling 9.8 cm ² of area per strand. The yield stress is 1,860 MPa.	
Prestressing steel	Y1860S7, $f_{pk} = 1860\text{N/mm}^2$, low relaxation steel (EN 10138-3: "Prestressed steels - Part 3: Wire")	
Bridge deck	Concrete C35/45 XC4 (P)	
Pavement	Asphalt	
Relaxation of prestressing steel strands at 1000 hours and 20°C (ρ_{1000h})		
Initial stress	Cordage (<i>Cordalha</i>)	
	Low relaxation (%)	Normal Relaxation (%)
0.5 f_{ptk}	0.00	0.00
0.6 f_{ptk}	1.30	3.50
0.7 f_{ptk}	2.50	7.00
0.8 f_{ptk}	3.50	120
RN: of wires and cords under tension after 1000 hours at 20°C (ρ_{1000h}).		

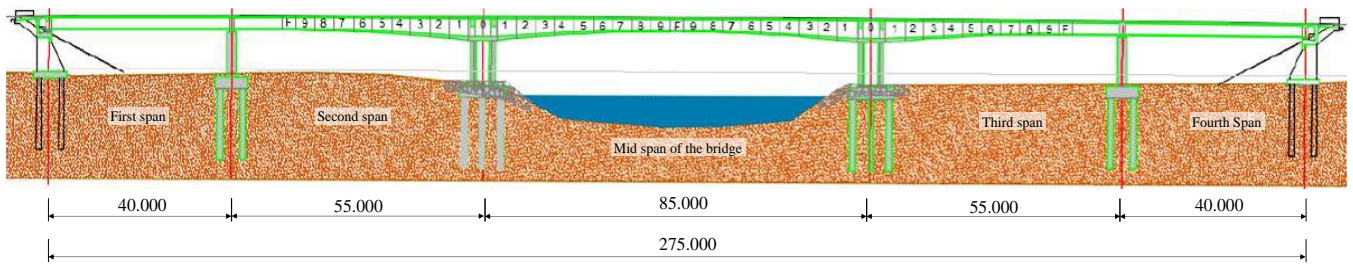
Source: Authors.

4. Case Study

4.1 Two Numerical Models

Two numerical models were developed, the first of which was intended for the construction phase of the bridge, where stresses were analysed in the sequence of all phases. The second (model) was intended for structural analysis during the operational phase of the bridge in question. As an illustration for better understanding, Figure 3 shows the longitudinal profile, as well as all current staves measuring 4.20 m each; the zero staves measuring 6.40 m and the closing staves measuring 3.0 m.

Figure 3 - Longitudinal profile and distribution of spans with respective dimensions (Unit: mm).



Source: Authors.

As can be seen in the figure above (Figure 3), the staves are highlighted with the numbers 0 to 9, which in turn corresponds to each construction phase. In the case of the segment “F” (in the middle of the span of the bridge) it represents the closure of the pairs of cantilevers. It can also be seen that the bridge will be built on two work fronts, with pairs of consoles being built symmetrically from the two central pillars. Then, in Table 2, the main parameters that constitute the materials used in the global model of the bridge are shown in detail below.

Table 2 - Main material parameters.

Structures	Materials	Modulus of elasticity (MPa)
Pillars	C50	50×34.5
Bridge deck	C55	55×35.5
Cable	Steel tensioner**	475.00

High strength prestress steel tensioner with 1,860.00 MPa tensile strength (similar to ASTM A416/A416M).

Source: Authors.

4.2 Reinforced Concrete Bridge Structural Project

The cross-section of the artwork was pre-dimensioned based on the Schlaich proposal (Morim, 2008 and Chai et al., 2019). Next, the dimensions of the box section of the bridge beam are shown in Figure 2. Highlighting that the height of the box beam section (at the supports) in the case study is determined according to the mathematical formulation expressed in Equation 1 (Morim, 2008).

As can be seen, the webs of the box beam were assumed to be maintained at a constant inclination and with a consequent variation in the width of the lower chord depending on the height. The inclination decision was adopted with the aim of providing less self-weight by reducing the width of the lower flange and a smaller transverse span in the section, thus favouring its rigidity. Table 3 shows the cross-sectional dimensions of each staff that makes up the bridge.

Table 3 - Dimensions of the cross-section of each stave that make up the bridge.

Stave s	h (m)	Minimum thickness (m)						Slenderness of the flanges (m)							i (m/m)
		t ₁	t ₃	t ₄	t ₅	t ₆	t ₇	b ₁	b ₂	b ₃	b ₄	b ₅	b ₆	b ₇	
0	4.79	0.18	0.25	0.45	0.45	0.75	1.00	2.75	7.00	3.70	1.20	6.10	4.91	0.55	0.123
1	4.79	0.18	0.25	0.45	0.45	0.75	1.00		7.00	3.70	1.20	6.10	4.91	0.55	0.123
2	4.35	0.18	0.25	0.45	0.45	0.69	0.94		7.00	3.70	1.20	6.10	4.85	0.55	0.123
3	3.91	0.18	0.25	0.45	0.45	0.63	0.88		7.00	3.70	1.20	6.10	5.13	0.55	0.123
4	3.68	0.18	0.25	0.45	0.45	0.57	0.82		7.00	3.70	1.20	6.10	5.18	0.55	0.123
5	3.41	0.18	0.25	0.45	0.45	0.51	0.76		7.00	3.70	1.20	6.10	5.24	0.55	0.123
6	3.10	0.18	0.25	0.45	0.45	0.44	0.69		7.00	3.70	1.20	6.10	5.32	0.55	0.123
7	2.90	0.18	0.25	0.45	0.45	0.38	0.63		7.00	3.70	1.20	6.10	5.37	0.55	0.123
8	2.70	0.18	0.25	0.45	0.45	0.32	0.57		7.00	3.70	1.20	6.10	5.42	0.55	0.123
9	2.59	0.18	0.25	0.45	0.45	0.26	0.51		7.00	3.70	1.20	6.10	5.44	0.55	0.123
F	2.59	0.18	0.25	0.45	0.45	0.20	0.45	7.00	3.70	1.20	6.10	5.44	0.55	0.123	

h - Section height; i - Inclination of web. Source: Authors.

4.3 Quantification of the Actions Considered

The actions were considered to be those of a permanent nature (self-weight of the staves and other fixed components of the bridge, as well as the own weight of the assembly aid equipment) and of a variable nature, which in this case are road overloads and wind action.

Permanent loads were calculated by multiplying the cross-sectional area of the element by the specific weight of the respective material that constitutes it. Table 4 presents some geometric properties and self-weight of the bridge staves.

Table 4 - Properties and self-weight of the bridge staves.

Staves	h (m)	e _{inf} (m)	A (m ²)	\tilde{y} (m)	I (m ⁴)	W _{inf} (m ³)	W _{sup} (m ³)	P (kN/m)
0	4.79	0.75	12.272	2.41	42.317	17.559	17.780	306.79
1	4.79	0.75	12.272	2.41	42.317	17.559	17.780	306.79
2	4.35	0.69	11.629	2.22	32.998	14.864	15.492	290.73
3	3.91	0.63	10.975	2.03	25.004	12.317	13.300	274.36
4	3.68	0.57	10.467	1.95	21.05	10.795	12.167	261.68
5	3.41	0.51	9.923	1.84	16.983	9.230	10.817	248.06
6	3.10	0.44	9.282	1.72	12.906	7.503	9.352	232.06
7	2.90	0.38	8.781	1.65	10.477	6.350	8.382	219.51
8	2.70	0.32	8.274	1.59	8.308	5.225	7.485	206.85
9	2.59	0.26	7.853	1.57	6.996	4.456	6.859	196.32
F	2.59	0.20	7.512	1.63	6.378	3.913	6.643	187.81

Source: Authors.

The weight of the remaining pressing loads (asphalt, curb, border beam and guardrails) were calculated taking into account the respective cross-sectional areas and multiplied by two, in order to mirror their existence on both sides of the section.

Table 5 shows the values of the areas, as well as the remaining permanent loads.

Table 5 - Remaining permanent loads.

Structural Elements	γ (kN/m ³)	A (m ²)	P (kN/m)
Asphalt	23.0	0.6802	15.64
Curb	25.0	0.255 0	6.38
Tours	12.0	0.7916	9.50
Edge beams	25.0	0.2932	7.33
Guard - Body	25.0	0.1924	4.81
		ΣR_{cp}	43.66

Source: Authors.

The bridge's road overloads were quantified according to Eurocode 1 – part 2 (2010). They were defined by the application of two uniformly distributed loads: 9.0 kN/m² on the first lane and 2.5 kN/m² on the remaining lanes, and concentrated loads spaced 2.0 m apart, 300 kN and 200 kN for the first and the second track respectively. A crowd load of 5.0 kN/m² was considered, taking into account that when producing vibrations with a frequency equal to that of the bridge, they can lead to structural collapse.

In the construction phase, overloads arising from the weight of all auxiliary equipment for the execution of the deck were considered. However, a mobile load with a total weight of 500.0 kN was defined, lower than the weight of the closing rod (563.43 kN) according to the recommended weight value. The remaining equipment is given by an evenly distributed overload of 0.50 kN/m². As for the wind action, it was quantified based on the European standard Eurocode 1 – part 4 (2010), having obtained the loads in each direction, being 11.528 kN/m, 2.882 kN/m and 11.277 kN/m, in the X, Y, Z directions respectively, as presented in Table 6. Furthermore, the combination and reduction factors considered in the variable actions are presented in the same table.

Table 6 - Wind actions in each direction and combination factors, and the reduction of variable actions.

Wind strength (kN/m)	Combination factors	Variable Action					
		S _{b_V}	S _{b_M}	V _(x)	V _(y)	V _(z)	
F _{w(x)}	11.528	ψ_0	0.60	0.40	0.40	0.40	0.40
F _{w(y)}	2.882	ψ_1	0.40	0.30	0.20	0.20	0.20
F _{w(z)}	11.277	ψ_2	0.20	0.20	0.00	0.00	0.00

S_{b_V}, S_{b_M} – Action due to road overload of vehicles and crowds; V_x, V_y e V_z – Action due to the force of the wind. Source: Authors.

For the operational phase, three combinations were defined for checking the Ultimate Limit State (“ELU”) and another three for the Service Limit State (“ELS”), with the vehicle overload being the most variable and influential action, taken with greater attention, as shown in Table 7. The combinations for “ELU” and “ELS” are expressed mathematically according to Equations 1 and 2, respectively (EC1 – part 4, 2010). It is worth highlighting that, in the case of “ELS”, quasi-permanent combinations were taken into account (long-term limit states – with a probability of occurrence greater than 50% of the structure’s useful life), as were also the frequent combinations (short-term limit states – with a probability of occurrence greater than or equal to 5% of the structure's useful life) and the rare combinations (limit state of very short duration - with probability of occurrence; a few hours of the structure's useful life), respectively. The nomenclatures of the equations were considered based

on Eurocode (EC1 – part 4, 2010).

$$F_d = \gamma_g F_{gk} + \gamma_q \left(F_{qk,1} + \sum_2^n \psi_{0,j} F_{q,k,j} \right) + \gamma_{\varepsilon q} \psi_{0\varepsilon} F_{\varepsilon q,k} \quad (1)$$

$$F_d = \sum_i^m F_{g,k,i} + \sum_2^n \psi_{2,j} F_{q,k,j} \quad ; \quad F_d = \sum_i^m F_{g,k,i} + \psi_1 F_{qk} + \sum_2^n \psi_{2,j} F_{q,k,j} \quad ; \quad F_d = \sum_i^m F_{g,k,i} + F_{qk,1} + \sum_2^n \psi_1 F_{q,k,1} \quad (2)$$

Table 7 - Multiplicity factors of variable actions.

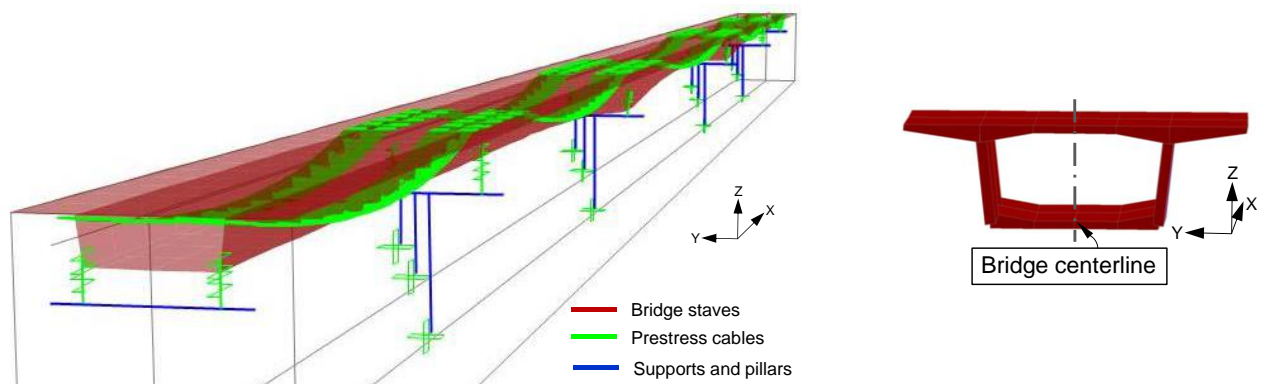
Case	Combination type	Description of the combination	Actions in the operational phase							
			PP	R _{cp}	PE	S _{b_v}	S _{b_M}	V _x	V _y	V _z
1	Normals (ELU)	AVB: S _{b_M}	1.35	1.35	1.20	0.90	1.50	0.60	0.60	0.60
2	Normals (ELU)	AVB: S _{b_v}	1.35	1.35	1.20	1.50	0.60	0.60	0.60	0.60
3	Normals (ELU)	AVB: V _x	1.35	1.35	1.20	0.90	0.60	1.50	0.60	0.60
4	C.Q.P. (ELS)	-----	1.00	1.00	1.00	0.20	0.20	0.00	0.00	0.00
5	Frequent (ELS)	AVB: V _x	1.00	1.00	1.00	0.20	0.20	0.20	0.00	0.00
6	Frequent (ELS)	AVB: S _{b_v}	1.00	1.00	1.00	0.40	0.20	0.00	0.00	0.00

AVB - Base variable action taken in each combination; PP - Action due to own weight; CM - Action due to the weight of the moving load; R_{cp} - Action due to remaining permanent loads; PE - Action due to prestress. Source: Authors.

4.4 Finite element model

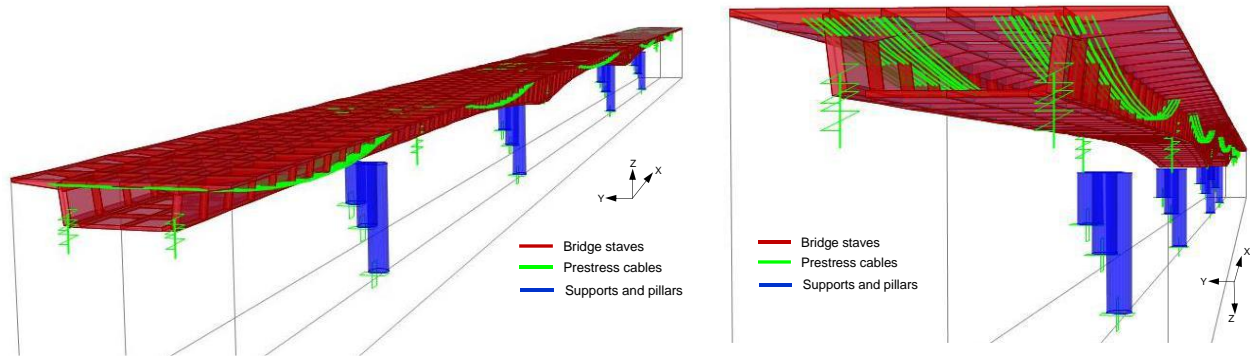
The computational numerical model (see Figure 4) developed in the CSiBridge program to evaluate the stresses and deformations (linear-static) of the reinforced concrete bridge adopted the usual mesh refinement techniques present in finite element method simulations implemented by others using this same software as well as in the Robot Structural 2018 program. The box beam and deck were modelled and simulated with area or shell finite elements. The pillars were simulated by bar-type elements. The global (final) model adopted used 17,261 elements, 18,453 nodes, resulting, therefore, in a numerical model with 91,082 Degrees of Freedom (GL). As for the damping rate, it was adopted as recommended in the standard EN 1991-2 (2003) for concrete bridges. Next, Figure 5 illustrates the different views of the model in order to illustrate its details.

Figure 4 - Overall model of the bridge highlighting the interior prestress cables adherent to the concrete.



Source: Authors.

Figure 5 - Different views of the global model of the reinforced concrete bridge.



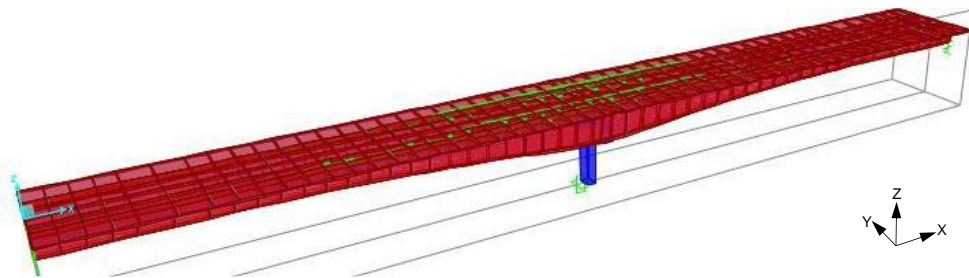
Source: Authors.

4.5 Model Used in the Construction Phase of the Bridge

As previously discussed, the CSiBridge program v.20 was adopted for the longitudinal analysis of the deck, taking into account the influence of the construction process and structural behaviour. In other words, two numerical models were developed; the first for the construction phase, as shown in Figure 6, and the second, intended for structural analysis during the operational phase of the bridge in question.

This first model was simplified to a single pair of consoles built symmetrically from a central pillar, reflecting the behaviour of the two work fronts, which will later be connected by closing staves. During the analysis of this construction process, the effects of creep, shrinkage, aging of the concrete, as well as the relaxation of the structural steel were taken into account.

Figure 6 - First numerical model – Used for the analysis during the construction phase.



Source: Authors.

The set of cables, which can also be called a family of pre-stressing cables defined to link each current stave, is made up of internal cables adherent to the concrete, with horizontal and straight lines, applied to the upper fibers of the section, as it is the zone where tensile stresses occur most frequently during the construction phase of the bridge.

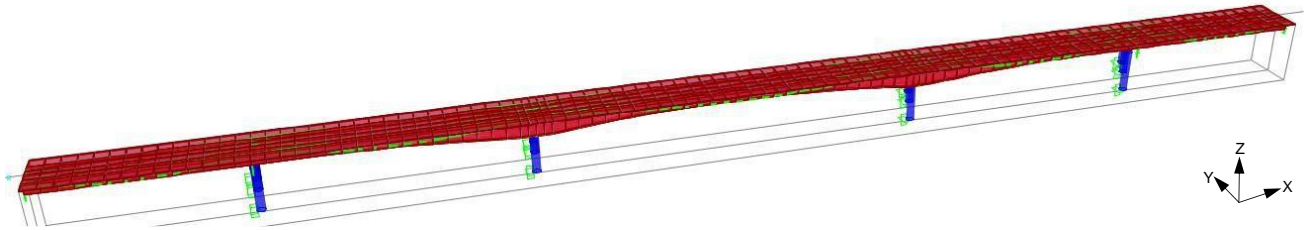
And in the case of consoles, the family of continuity cables were defined as internal prestress cables that adhere to the concrete, but with parabolic layouts, ensuring the connection between the two work fronts and introduced into the lower fibers of the section in order to overcome the tensile stresses that arise in this area, resulting from the redistribution of efforts, resulting from the change in the structural system, initially isostatic and then becoming a hyperstatic structural system.

4.6 Numerical Model Used in the Bridge Operation Phase

In the case of the second model developed, as illustrated in Figure 7, it was intended for carrying out structural analyses during the operational phase of the bridge in question.

In this second model, with the closure of all pairs of cantilevers, their 5 respective spans were considered, this being the numerical model (hyperstatic) adopted for the analysis and used for the operational phase of the bridge.

Figure 7 - Second numerical model – Analysis during the bridge operational phase.



Source: Authors.

It is important to highlight that, as in the first model, in this second model the curvature of the lower flange was defined parametrically, so as to obey a parabolic shape with specific heights for each stave. In the analysis process, geometric non-linearity as well as material non-linearity were taken into account. As for the effects of temperature and the effects of earthquakes or seismology, these were not considered, as they were not within the delimitation and/or objectives of the present research work.

4.7 Transverse Numerical Model of the Bridge Deck

A detailed analysis was necessarily carried out for the transverse direction of the deck, to determine an optimal sequence of application of the pre-stressing cables, in each of the phases, since the sequence in question consists of a process that influences and/or has a considerable impact on its stability, to the point that in some cases it generates excessive displacements and rotations when not applied judiciously, thus causing additional efforts in the structural system.

In this way, carrying out the transverse analysis on the deck makes it possible to assess whether or not it is necessary to apply a transverse prestress, depending on the efforts that will arise in the structure. To this end, the cross-section model in the support region was developed based on the aid of the finite element software Robot Structural Analysis, using bar elements. It is worth highlighting that the support regions are those where the greatest efforts arise or are perceived during the construction phase.

As expected, in the analysis process, the loads displayed in the model are related to the fixed elements which contribute to the permanent loads in the section. Therefore, the concentrated loads located at the ends, corresponding to 6.07 kN (F_z) reflect the border beams with the guardrails. The concentrated loads of 3.19 kN (F_z), located in the innermost area of the console, mirror the curb; and in the case of the uniformly distributed load in a linear way corresponding to 4.75 kN/m (P_z), these reflect the weights of the sidewalks (on both sides of the bridge), and the load of 1.25 kN/m (P_z) reflects the weight of the bituminous material, which is also known as asphalt.

5. Results and Discussion

The results were obtained for both the construction phase and the operational phase. Next, the maximum internal design forces obtained for the bridge deck in each phase are presented in Table 8. The values were taken from the most highly tensioned area (specifically in stave zero), for the application sequence of the prestress cables so they become structurally more efficient.

Table 8 - Maximum values of bridge design efforts.

Phase	Distance (m)	P (kN)	V _y (kN)	V _z (kN)	T (kN.m)	M _y (kN.m)	M _z (kN.m)
0	3.20	-3,168.79	228.63	361.39	299.79	2,199.28	-1,347.07
1	7.40	-5,816.09	240.17	358.87	377.11	2,834.01	-3,870.52
2	11.60	-8,392.64	211.46	343.69	324.33	3,477.62	-6,499.62
3	15.80	-8,401.49	230.85	474.73	404.10	2,262.09	-8,391.23
4	20.00	-10,640.00	191.42	472.67	433.72	2,745.81	-13,006.29
5	24.20	-13,298.74	169.88	497.21	416.96	2,995.08	-18,617.79
6	28.40	-13,370.19	198.50	504.73	509.38	2,147.14	-20,449.54
7	32.60	-16,002.12	190.82	455.62	594.36	1,160.12	-28,430.12
8	36.80	-18,564.90	204.14	414.26	751.31	698.10	-38,299.28
9	41.00	-22,459.25	250.00	397.66	202.85	1,020.34	-46,365.51
F	44.00	-21,125.01	190.823	247.89	189.97	962.48	-29,611.65

Source: Authors.

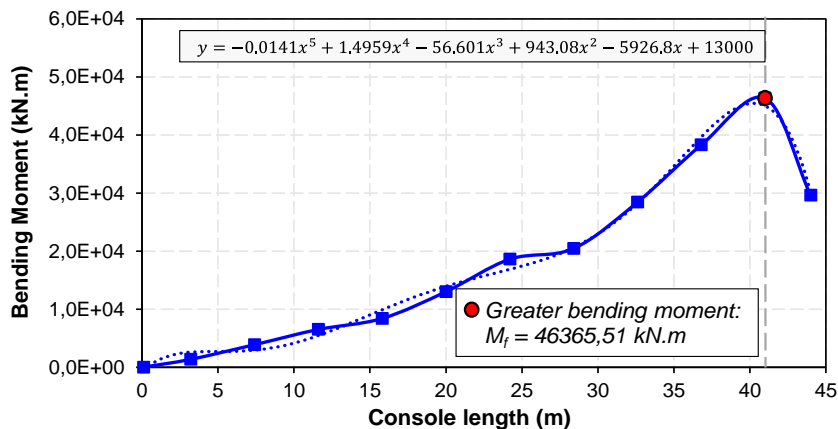
It can be seen that with the application of the pre-stress, the internal stresses are considerably reduced due to the opposite deformation imposed on the structure, but with the exception of the axial effort which increases, since the pre-stress contributes to the compression of the structure.

It is important to highlight that, after closing the two pairs of consoles (phase “F”), there was a redistribution of efforts, changing the maximum bending moment from a value of -46365.51 kN.m to a value of -29611, 65 kN.m, this is due to the change in the structural system, which was initially isostatic and became hyperstatic, consequently generating, in the middle span, a bending moment with a value of 7129.03 kN.m, after the removal of the assembly equipment, even before taking into account the actions of the operational phase of the bridge.

5.1 Evolution of Internal Efforts

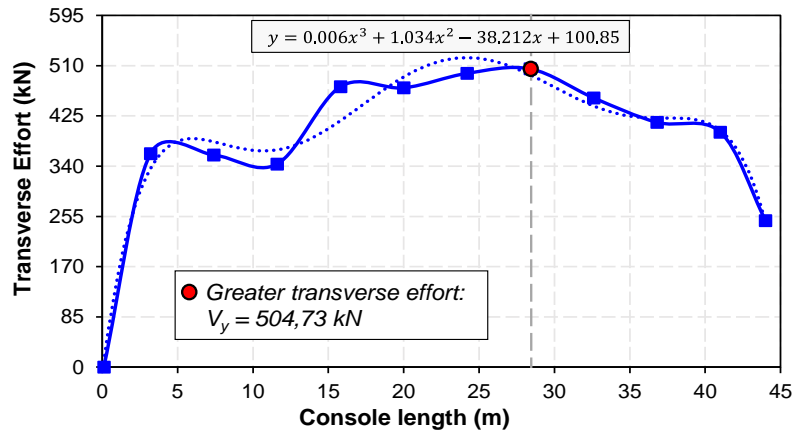
As can be seen, Figures 8, 9 and 10 present the results of the internal sizing efforts (bending moment, transverse effort and axial effort), obtained during the construction phase. It can be seen that the values in question grew in accordance with an approximate mathematical function, as the length of the cantilever pair increased (until reaching their maximum values in the phase prior to the closing of the staves).

Figure 8 - Evolution of the bending moment effort in the upper fibers of stave zero.



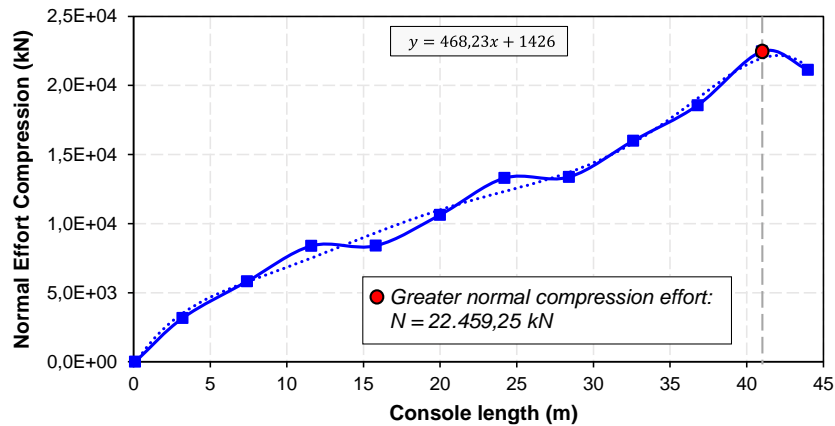
Source: Authors.

Figure 9 - Evolution of the maximum transverse force (shearing force) in stave zero.



Source: Authors.

Figure 10 - Evolution of the axial compression force in the structure.



Source: Authors.

In Figure 8, it can be seen from the bending moments graph (construction phase), that the values, represented by a fifth-degree polynomial, increase until the end of the construction phase. After the closure of the two pairs of consoles, there is a redistribution of efforts resulting from this new phase of the project. In this context, the evolution of the bending moment in the construction phase follows an increasing average rate per 4.2 m of 1920.46 kN.m.

In the case of the growth of the transverse effort (shear force shown in Figure 9) in the phase in question, the values can be represented by a third-degree polynomial. These are greatly influenced by the curvature of the lower flange and the reduction of the sections along the consoles (reduction of self-weight). The curvature of the lower flange considerably alleviates the effect of transverse stress due to the vertical component of the concrete stress.

In the case of the axial force results illustrated in Figure 10, these grow almost linearly during the construction phase, compressing mainly the upper fibers of the section, since the pre-stressing cables were introduced at the upper flange (consolidation cables) until shortly before closing the consoles (continuity cables – lower flange).

5.2 Pressurising Results Based on the Number of Cables

In Table 9, the values determined for the prestress based on the family of internal cables adherent to the concrete with straight lines are presented. It is highlighted that, for the continuity cables of the consoles, a family of internal cables adhering to the concrete was used, but with parabolic layouts, consisting of cords, each of them having 7 wires with nominal diameters of

15.0 mm and an area of 1.40 cm² as recommended by ASTM - *American Society for Testing and Materials* (ASTM, 1998), having, however, a total area of 9.80 cm² subject to a tension of 1,860 MPa.

Table 9 - Efforts determined for pre-stress.

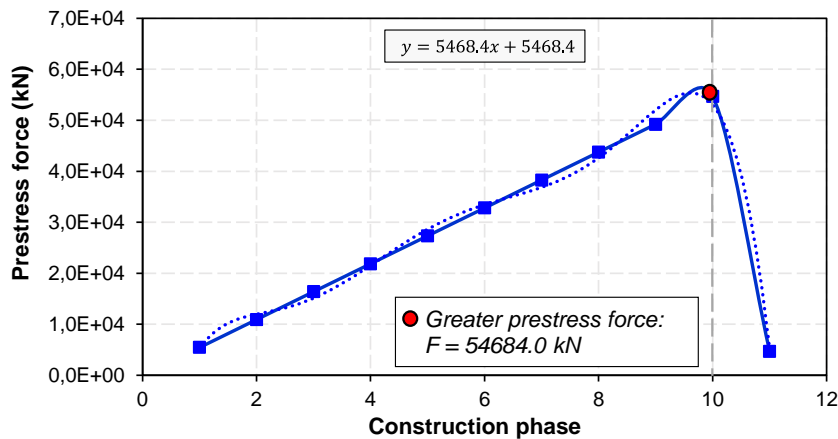
Phase	New stave		Zero stave		Prestress force
	N° Cables	A (cm ²)	N° Cables	A (cm ²)	F (kN)
0	4	39,20	4	39.20	5468.40
1			8	78.40	10936.80
2			12	117.60	16405.20
3			16	156.80	21873.60
4			20	196.00	27342.00
5			24	235.20	32810.40
6			28	274.40	38278.80
7			32	313.60	43747.20
8			36	352.80	49215.60
9			40	392.00	54684.00
F	6	58,8	---	---	4687,20

Source: Authors.

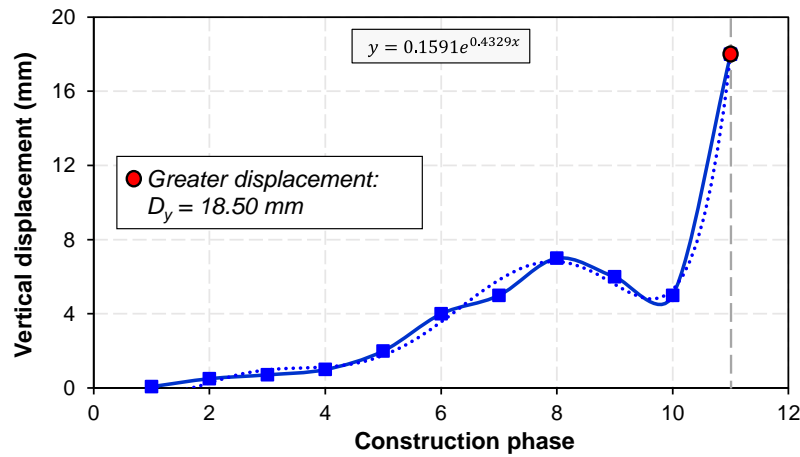
As can be seen in the previous table (Table 9), the construction of stave zero was carried out with 4 cables, and the others were built by successively adding 4 new cables (respectively). As for the force applied to the pre-stress, it increases with each new construction phase, thus following the growth of internal efforts. The way in which the application force increases depending on the construction of the consoles (staves), as well as the behaviour of the bridge in terms of displacements, is then presented in graphic form in Figure 11.

As can be seen, the pre-stress force increases linearly until the phase prior to the closing of the cantilever pairs. However, based on the increase in tensile stresses, there is obviously a need to increase the number of cables, in order to guarantee a larger pre-stress area, thus reducing possible prestress losses. The decay seen during the stave closing phase is due to the fact that, at this stage, the pre-stress cables to be applied are those of continuity, that is, in the lower fibers, in order to overcome the tensions that arise there as a consequence of the redistribution of efforts also ensuring continuity between consoles. These tensions, in turn, are smaller compared to those that arise in the upper fibers, hence the need to apply a lower prestress force.

Figure 11 - Evolution of the axial compression force in the structure.



(a)

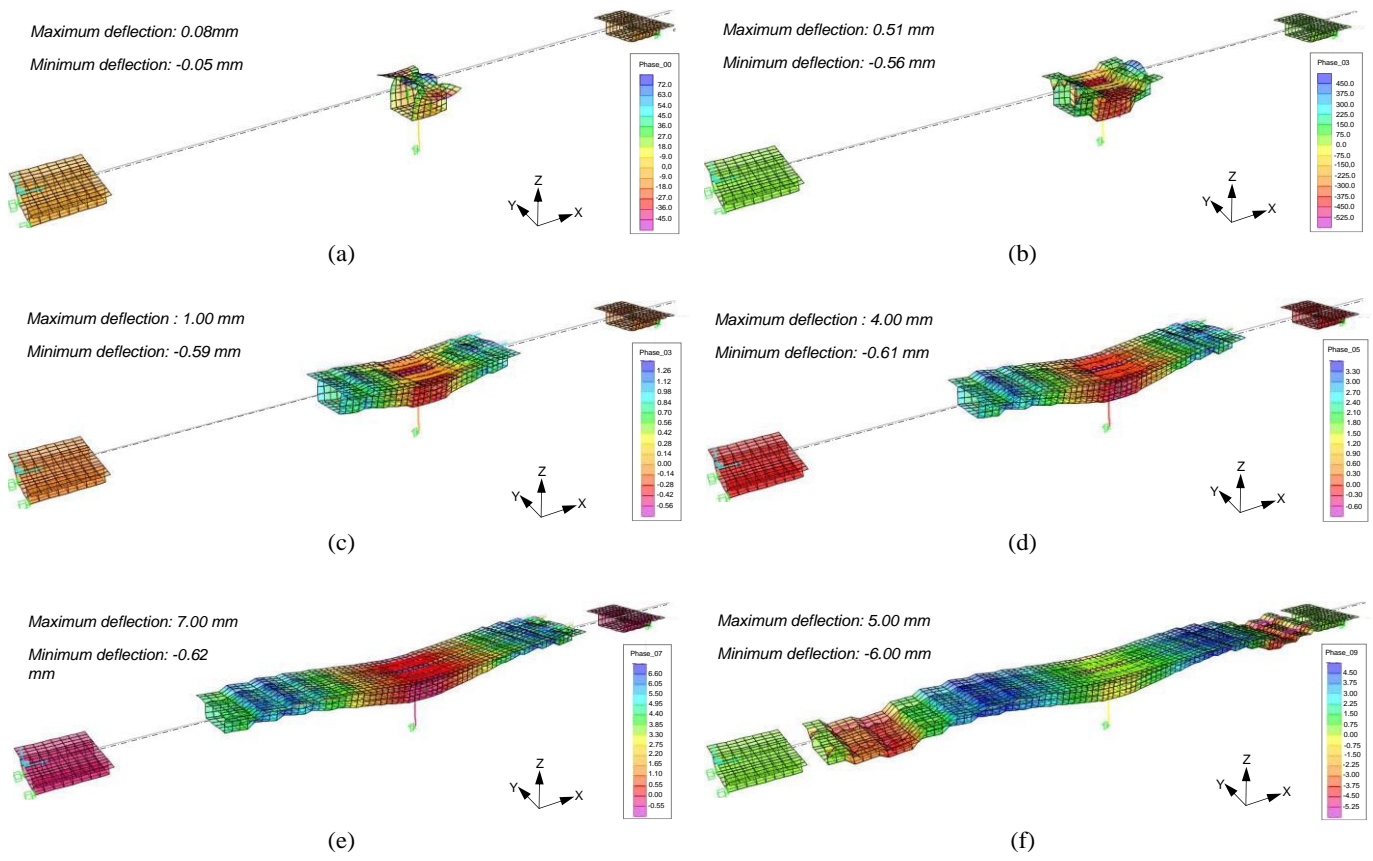


(b)

Source: Authors.

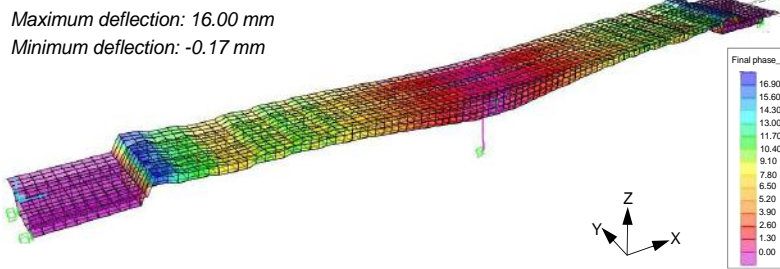
Regarding the application of pre-stress cables in the structural system, it is highlighted that three different application sequences of pre-stress cables were considered and carried out in order to verify their efficiency and influence on the structural behaviour in terms of displacements and deck rotations, as well as internal sizing efforts. In this context, the results presented in this research are only those that demonstrate the best cable application sequences and consequently greater efficiency regarding the behaviour of the bridge, considering that the cable sequence in question is managed to generate smaller deformations and, consequently lower internal efforts. Figure 12 then illustrates the sequence of application of the staves and their respective deformations. Figure 13, finally illustrates the deformed state of the bridge deck; and below, the displacements and rotations of the deck during the construction of the bridge are illustrated in Figure 14, in a graphical form.

Figure 12 - Evolution of the axial compression force in the structure.



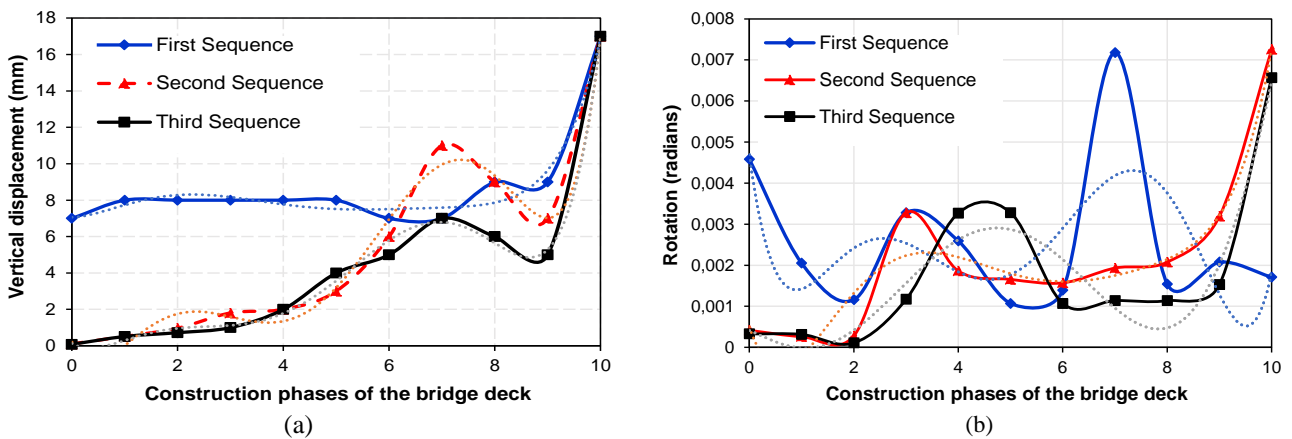
Source: Authors.

Figure 13 - Evolution of the axial compression force in the structure.



Source: Authors.

Figure 14 - Evolution of displacements and rotations of the bridge deck; a) displacements; b) rotations.



Source: Authors.

As discussed, the displacements in the three sequences gradually increase, resulting in a sudden change in the “Closing” phase of the consoles, as a result of the increase in internal efforts, caused by the redistribution of forces resulting from the change in the structural system. And in the case of rotations, with oscillatory behaviour, these had little influence at a structural level, since their values are very close to zero, which translates into good transverse stability in the defined section and in the way in which the prestressing cables were applied. Considering the structural behaviour, it can be clearly observed (see Figure 14) that the results defined by the third sequence of cables are predominantly lower than the results of the first sequence. This efficiency is due to the alternating application and concentration of cables from the initial and final phases (0, 1 and 9) in areas of greater cross-sectional effort (inclined webs), which are also, in turn, the areas that give it greater rigidity.

5.2.1 Results of Internal Efforts in the Operational Phase

In addition to the loads applied during the construction phase of the bridge (the actions of the self-weight of the staves and the remaining permanent loads), the road overloads in accordance with the Eurocode, the wind forces in the three directions (“X”, “Y” and “Z”) and the vehicle type loads and the prestress were applied during the operational phase. Table 10 presents the internal forces obtained during the operational phase of the bridge, taking into account the most critical/unfavourable combinations, both from the point of view of checking the Ultimate Limit State (ELU) and the Service Limit State (ELS), described in the table as COMB_2 and COMB_6, respectively.

It should be noted that the results in question, based on the use of the CSiBridge v.20 software, were obtained in the areas/regions of the internal supports, at the end supports and in the middle of each span as well, as these are the most highly tensioned areas. As expected, the efforts in question are greater than those obtained in the construction phase (after the redistribution of the efforts), due to the influence of all the operational loadings.

Table 10 - Internal efforts obtained in the operational phase of the bridge – CSiBridge v.20.

Distance (m)	COMB_2						COMB_6					
	P (kN)	V _y (kN)	V _z (kN)	T(kN.m)	M _y kN.m)	M _z (kN.m)	P (kN)	V _y (kN)	V _z (kN)	T(kN.m)	M _y (kN.m)	M _z (kN.m)
0.00	-4.8E+04	4.4E+03	4.0E+02	4.2E+03	7.1E+03	5.8E+04	-3.9E+04	4.6E+03	3.0E+02	3.1E+03	5.3E+03	5.0E+04
17.14	-5.2E+04	2.7E+03	4.0E+02	4.2E+03	2.5E+02	-2.0E+03	-4.2E+04	2.3E+03	3.0E+02	3.1E+03	7.8E+01	-8.4E+03
40.00	-4.5E+04	1.4E+04	4.0E+02	4.2E+03	-8.9E+03	-2.9E+04	-3.7E+04	1.0E+04	3.0E+02	3.1E+03	-6.8E+03	-1.7E+04
68.49	-3.9E+04	5.8E+03	3.0E+01	7.1E+03	-6.0E+03	-6.5E+04	-3.1E+04	4.2E+03	2.4E+01	5.2E+03	-4.4E+03	-5.3E+04
95.00	-3.4E+04	2.6E+04	3.0E+01	7.1E+03	-6.8E+03	-3.2E+05	-2.7E+04	1.9E+04	2.4E+01	5.3E+03	-5.1E+03	-2.3E+05
137.50	-3.1E+04	-2.8E+02	-1.7E+01	1.4E+00	-7.9E+03	9.0E+04	-2.5E+04	-2.4E+02	-1.4E+01	1.2E+01	-5.8E+03	6.4E+04
180.00	-2.8E+04	2.9E+04	-1.7E+01	-1.1E+01	-7.2E+03	-3.4E+05	-2.2E+04	-2.0E+04	-7.6E+01	-5.3E+02	-6.4E+03	-2.4E+04
206.51	-2.5E+04	-4.7E+03	-9.3E+01	-7.0E+03	-5.9E+03	-5.2E+04	-1.9E+04	-3.3E+03	-7.6E+01	-5.2E+03	-4.4E+03	-4.2E+04
235.00	-2.3E+04	-1.4E+04	-4.5E+02	-4.2E+03	-1.1E+04	-5.3E+04	-1.8E+04	-1.0E+04	-3.5E+02	-3.1E+03	-8.5E+03	-3.7E+04
255.00	-2.0E+04	-2.1E+03	-4.5E+02	-4.2E+03	-1.8E+03	3.6E+04	-1.5E+04	-1.6E+03	-3.5E+02	-3.1E+03	-1.6E+03	2.4E+04
275.00	-8.4E+03	4.4E+03	-4.5E+02	-4.2E+03	7.2E+03	2.8E+04	-5.8E+03	2.8E+03	-3.5E+02	-3.1E+03	5.4E+03	2.5E+04

Source: Authors.

As can be seen, combinations 2 and 6 (COMB_2 and COMB_6) highlighted the largest and smallest efforts in the longitudinal direction “Z”. Therefore, it is concluded that the most unfavourable efforts are provided in the COMB_2 combination. In the transverse direction, based on the application of the Robot Structural software, the most critical values were obtained, resulting in: -733.76 kN.m and 562.14 kN.m (bending moments); -49.06 kN and 531.64 kN (shearing/transverse forces); 0.0 kN and 635.88 kN (normal efforts), minimum and maximum, respectively.

5.2.2 Results of Deck Deformations in the Operational Phase

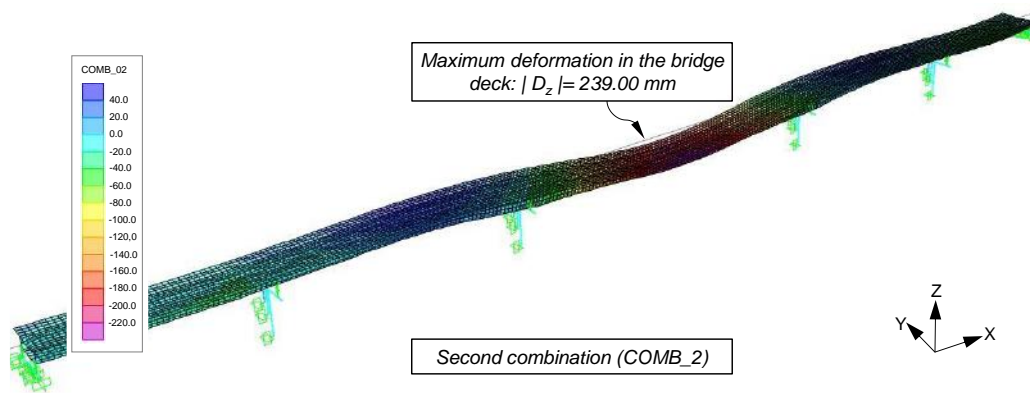
The results of the maximum and minimum deformations of the deck in the operational phase, taking into account the most critical/unfavourable combinations (COMB_2 and COMB_6), are presented in Table 11. Next, the deformed states of the deck in the direction “Z”.

Table 11 - Maximum and minimum deformations in the operational phase.

Case	D _x (mm)	D _y (mm)	D _z (mm)	R _x (radians)	R _y (radians)	R _z (radians)
COMB_2	12.05	2.32	53.00	-1.80E-04	5.34E-03	9.34E-04
	-17.12	-28.14	-239.00			
COMB_6	10.04	1.31	41.00	1.08E-04	9.54E-03	-7.80E-03
	-13.20	-21.02	-173.00			

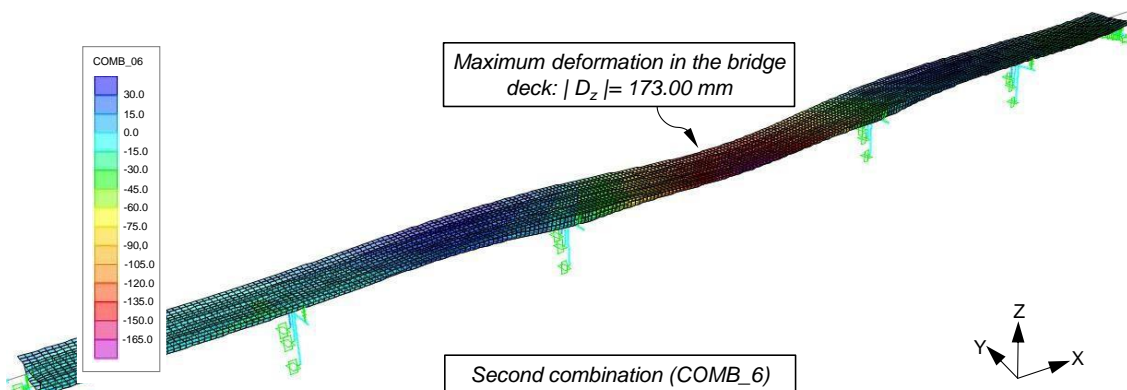
Source: Authors.

Figure 15 - Deformed state of the bridge deck – COMB_2.



Source: Authors.

Figure 16 - Deformed state of the bridge deck – COMB_6.



Source: Authors.

5.2.3 Results of Prestress Losses

As for the results referring to pre-stress losses in areas with higher tensile stresses (the middle of each span) taking into account the combinations that provide the greatest efforts, these (results) are presented in detail in Table 12.

In this context, the loads identified as P_{\min} (in Table 12) correspond to the minimum loads which guarantee no decompression in the section where the pre-stress is applied. The P_{apl} value corresponds to the load that will be applied, which must always exceed P_{\min} . According to the regulatory technical recommendations this value, even after all the losses (immediate and deferred), must still be larger than P_{\min} . It can be seen from the table in question that the greatest prestressing losses are acceptable since they add up to less than the 15%, which were considered in the design.

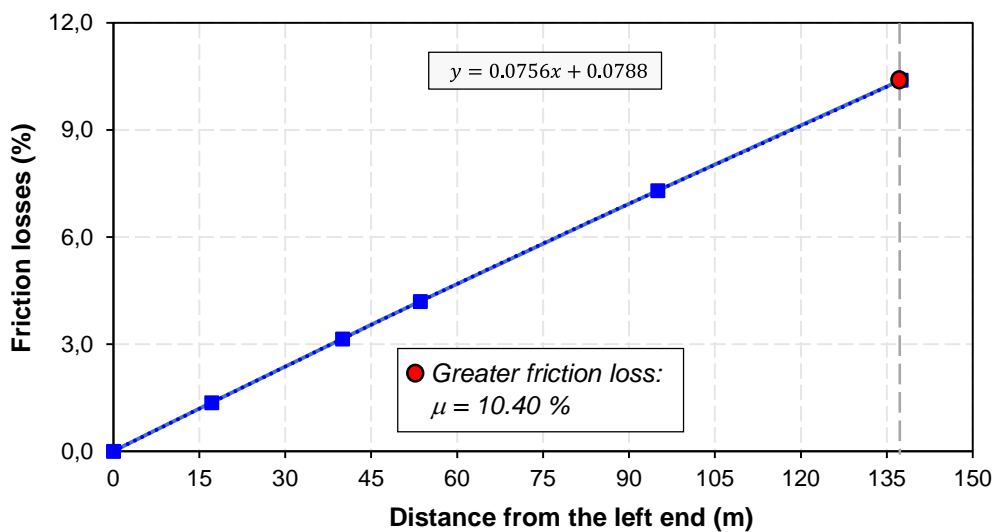
Table 12 - Prestressing losses due to friction taking into account eccentricity.

Distance (m)	e_i^* (m)	Critical cases	M (kN.m)	P_{\min} (kN)	P_{apl} (kN)	Prestress losses			
						Friction	Def. inst	Retraction	Fluency
0.00	0.00	--	0.00	0.00	0.00				
17.14	1.55	COMB_1	28441.60	13734.30	21873.60	1.36			
40.00	0.79	COMB_2	28581.60	17070.40	32810.40	3.15			
53.59	1.51	COMB_2	4182.91	1953.23	43747.20	4.20	0.39%	2.13%	0.69%
95.00	2.26	COMB_4	126743.00	34172.70	54684.00	7.30			
137.50	1.51	COMB_3	58090.9	28604.40	54684.00	10.40			

*Eccentricity. Source: Authors.

As can be seen in Figure 17, the pre-stress losses due to friction develop linearly, following a growth rate of around 6.48% of the initial value, which occurs mainly in longer cables, specifically and or above all, in the middle of the central span of the bridge.

Figure 17 - Friction losses in the domain of distances in meters.



Source: Authors.

6. Conclusions and Suggestions for Future Work

The main objective of this research work was to investigate the structural behaviour of a box-type reinforced concrete road bridge, which was designed using the method of successive advances, in order to evaluate its deformations (following the application of pre-stress during construction) having tensile stresses in the upper fibres of the webs. Based on this study it was possible to reach the following conclusions:

- The variation in the arrangement in the form of sequence of application of the pre-stress cables leads to considerable changes in deformations and, consequently, in the internal efforts in the structural system, since the order of the cables influences above all the transversal stability of the section, which can create situations of imbalance, when poorly applied, thus increasing rotations and displacements in the structure.
- Among the defined sequences of application of prestress cables, where the cables were applied alternately between the most rigid and least rigid areas of the section in study, proved to be most efficient in terms of structural behaviour. In other words, it is the most efficient sequence in terms of the fact that it generates smaller deformations and, consequently, smaller internal efforts.
- With the closure of the pairs of consoles, built symmetrically in two work towers, there was a redistribution of internal efforts, reducing them considerably. Regarding the bending moment there was a reduction of 36.13%, for the transverse force a reduction of 37.66% and for the axial force a reduction of 5.94%.
- Given the constraints of the calculation model, as expected, the transverse effort values were not high enough to require transverse pre-stress, thus verifying that with the curvature defined for the lower flange, it was possible to alleviate its effect due to the contribution of the vertical component of the concrete stress.
- With the definition of straight lines for the pre-stress cables which join the staves, it was possible to significantly reduce friction losses, with the highest value being 10.40%. This due, mainly, to the fact that the prestress force values applied were much higher than those strictly necessary for the decompression of the section to be avoided.
- As shown in the last graph, of friction losses as a function of distance, it is possible to conclude that the instantaneous prestress losses due to friction developed along the bridge deck grow linearly at a rate of 6.48% of their application value (of the initial value), and this occurs in longer cables.

During the course of this research, several research perspectives emerged that deserve future attention. Therefore, as suggestions for future work, some research topics can be developed some posteriori, which are described below:

- Carry out a thorough analysis of the routing of internal efforts during the application of pre-stress.
- Study how the construction process influences structural behaviour at the level of infrastructure and meso-structure.
- Evaluate the other structural components of the bridge considering dynamic loads and track irregularities.
- Carry out a comparative analysis between the application of external prestress cables to concrete and internal cables adherent to structural concrete. The analysis for different layouts (polygonal, horizontal and parabolic cables).
- Carry out dynamic monitoring of the structural components of bridges, in order to refine the computational analysis approach developed in the present research, and compare with the experimental approach.

References

- Almeida, I. D. A. (2016). *Segurança de Pontes na Fase Construtiva*. Instituto Superior de Engenharia de Lisboa. Departamento da Engenharia Civil. 79.
- American Society for Testing and Materials. (1998). "ASTM E606-92: Standard Practice for Strain-Controlled Fatigue Testing", In *Annual Book of ASTM Standards, Part 11*, 557-581.
- Associação Brasileira de Normas Técnicas, ABNT NBR 7187 (2021). *Projeto de pontes de concreto armado e de concreto protendido*.
- Barbaros, A., Rafiullah, G., Tayfun, D., & Sevket, A. (2022). The effect of post-tensioning force and different cable arrangements on the behavior of cable-

stayed bridge. *Structures*, 44, 1824–1843.

Bakht, B. & Mufti, A. (2015). *Bridges analysis, design, structural health monitoring, and rehabilitation*. Springer.

Bakht, B. & Jaeger, L. G. (1985). *Bridge analysis simplified*. McGraw Hill Book Company.

Briseghella, B., Fa, G., Aloisio, A., Pasca, D., He, L., Fenu, L., & Gentile, C. (2021). Dynamic characteristics of a curved steel-concrete composite cable-stayed bridge and effects of different design choices. *Structures*, 34, 4669–4681.

Cardoso, J. M. D. L. B. (2014). Ponte de Concreto Protendido com Seção Caixaõ: Estabelecimento de Relação entre a Altura da Seção Transversal e o Vão. Escola de Engenharia da Universidade Federal do Rio Grande do Sul. Departamento de Engenharia Civil. Porto Alegre, p. 97.

Cardoso, J. M. L. B., Rios, R. D., & Molin, D. C. C. D. (2015). Ponte de concreto protendido com seção caixaõ: estabelecimento de relação entre altura da seção transversal e vão utilizando concreto de alto desempenho – Classe II – segundo a nova ABNT NBR6118/2014. ANAIS DO 57º CONGRESSO BRASILEIRO DO CONCRETO - CBC2015 – 57CBC.

Chai, T. S., Guo, Chen, Z. H., & Yang, J. (2019). Monitoring and simulation of long-term performance of precast concrete segmental box girders with dry joints. *J. Bridge Eng.*, 16, 0501613.

Cheng, X., Nie, X., & Fan, J. S. (2016). Structural Performance and Strength Prediction of Steel-to-Concrete Box Girder Deck Transition Zone of Hybrid Steel-Concrete Cable-Stayed Bridges. *J. Bridge Eng.*, 21, 04016083.

Da Silva, A. C. S., Quissanga, V., & Silva, J. G. S. (2023). Steel-concrete composite highway bridges dynamic structural behaviour assessment considering the pavement progressive deterioration effect. *IBRACON Structures and Materials Journal*. 16, 4, e16404. <https://doi.org/10.1590/S1983-41952023000400004>.

Davide, R.I., Vanni, N., Davide, A., Sandro, C., Fabrizio, G., & Luigino, D. (2022). A Good Practice for the Proof Testing of Cable-Stayed Bridges. *Appl. Sci.*, 12, 3547.

Fatemi, S. J., Ali, M. S., & Sheikh, A. H. (2016). Load distribution for composite steel-concrete horizontally curved box girder bridge. *J. Constr. Steel Res.*, 116, 19–28.

Huang, D.W., Wei, J., Liu, X.C., Xiang, P., & Zhang, S.Z. (2019). Experimental study on long-term performance of steel-concrete composite bridge with an assembled concrete deck. *Constr. Build. Mater.*, 214, 606–618.

Motter, D. D. C., Oliveira, F. C. D., & Xocaira, R. O. (2018). *Pontes e Viadutos – Balanços Sucessivos Com Aduelas Pré-moldadas*. Faculdade de Ciências Exatas e de Tecnologia da Universidade Tuiuti do Paraná. Curitiba, p. 17.

Paixão, R. D. O. D. (2015). Análise Mecânica e Estrutural de Balanços Sucessivos Aplicados à Construção de Pontes. Escola de Engenharia da Pontifícia Universidade Católica do Rio de Janeiro. *Departamento de Engenharia Mecânica*. Rio de Janeiro, p. 69.

Quissanga, V., Alencar, G. De Jesus, A., Calçada, R., & Silva, J. G. S. (2021). Distortion-Induced Fatigue Reassessment of a Welded Bridge Detail Based on Structural Stress Methods. *Metals*. 11(12):1952.

Quissanga, V. (2022). Análise estrutural dinâmica e verificação de projeto à fadiga de pontes rodoviárias em aço e mistas (aço-concreto). Universidade do Estado do Rio de Janeiro (UERJ). Rio de Janeiro, Brazil. 311, 201–258.

Reis, A. C., & Peres, G. L. (2016). O Método dos Avanços Sucessivos, desde a Fase de Projeto à Construção da Ponte. Faculdade de Ciências e Tecnologia da Universidade Nova de Lisboa. Lisboa, p. 97.

Zhou, G. P., Li, A. Q., Li, J. H., Duan, M. J., Xia, Z. Y., & Zhu, L. (2019). Determination and Implementation of Reasonable Completion State for the Self-Anchored Suspension Bridge with Extra-Wide Concrete Girder. *Appl. Sci.* 9, 2576.